Check for updates

Quantitative assessment of the choroidal vasculature in myopic macular degeneration with optical coherence tomographic angiography

Yee Shan Dan[1†], Kai Xiong Cheong[1†], Shen Yi Lim[1], Qiu Ying Wong[1], Rachel S. Chong[1,2], Chee Wai Wong[1*‡] and Quan V. Hoang[1,2,3,4*‡]

[1]Singapore Eye Research Institute, Singapore National Eye Centre, Singapore, Singapore, [2]Ophthalmology & Visual Sciences Academic Clinical Program (Eye ACP), Duke-NUS Medical School, Singapore, Singapore, [3]Department of Ophthalmology, Yong Loo Lin School of Medicine, National University of Singapore, Singapore, Singapore, [4]Department of Ophthalmology, Edward S. Harkness Eye Institute, Columbia University Vagelos College of Physicians and Surgeons, New York City, NY, United States

Background: To assess and compare choroidal morphometric vascular parameters, using optical coherence tomographic angiography (OCTA), in highly myopic adults with and without myopic macular degeneration (MMD).

Methods: This is a clinic-based observational study of 148 eyes with axial length (AL) $\geq$25mm, enrolled from the high myopia clinic of the Singapore National Eye Centre. MMD was graded from fundus photographs. Swept source OCT (SS-OCT) and OCTA were performed and assessed for choroidal layer thickness (CT) and choroidal vasculature (choroidal vessel density (CVD), choroidal branch area (CBA) and mean choroidal vessel width (MCVW)) in the different choroidal layers (overall choroidal layer (CL), medium-vessel choroidal layer (MVCL), large-vessel choroidal layer (LVCL)).

Results: CT_{CL} (r=-0.58, p<0.001), CT_{MVCL} (r=-0.22, p=0.04), $MCVW_{CL}$ (r=-0.58, p<0.001), and CVD_{CL} (r=-0.19, p=0.02) were negatively correlated with AL, while CBA_{CL} (r=0.61, p<0.001) was positively correlated. Compared to eyes with no MMD, eyes with MMD2 had lower CT_{CL} (120.37$\pm$47.18µm vs 218.33$\pm$92.70µm, p<0.001), CT_{MVCL} (70.57$\pm$15.28µm vs 85.32$\pm$23.71µm, p=0.04), CT_{LVCL} (101.65$\pm$25.36µm vs 154.55$\pm$68.41µm, p=0.001) and greater CVD_{CL} (71.10$\pm$3.97% vs 66.97$\pm$3.63%, p<0.001), CVD_{MVCL} (66.96$\pm$2.35% vs 65.06$\pm$2.69%, p=0.002), CVD_{LVCL} (68.36$\pm$2.56% vs 66.58$\pm$2.88%, p=0.012), $MCVW_{MVCL}$ (6.14$\pm$0.34µm vs 5.90$\pm$0.35µm, p=0.007), and CBA_{CL} (12.69$\pm$1.38% vs 11.34$\pm$1.18%, p<0.001). After adjusting for age, thicker CT_{CL} (odds ratio (OR) 0.98, 95% confidence interval (CI) 0.97-0.99, p<0.001), CT_{MVCL} (OR 0.97 (0.94-0.99), p=0.002) and CT_{LVCL} (OR 0.97 (0.96-0.98, p<0.001) were significantly associated with lower odds of MMD2, while increased CVD_{CL} (OR 1.37 (1.20-1.55), p<0.001), CVD_{MVCL} (OR 1.39 (1.12-1.73), p=0.003), CVD_{LVCL} (OR 1.31 (1.07-1.60), p=0.009), CBA_{CL} (OR 2.19 (1.55-3.08), p<0.001) and $MCVW_{MVCL}$ (OR 6.97 (1.59-30.51), p=0.01) was significantly associated with higher odds of MMD2.

Conclusion: Decrease in choroidal vessel width, density and thickness, and an increase in vascular branching were observed in eyes with long AL. A thinner and denser choroid with greater branching area and vessel width, which may all be signs of hypoxia, were associated with greater odds of MMD2.

Introduction

Myopic macular degeneration (MMD) is a major cause of visual impairment and blindness globally. As high myopia and age are the major risk factors for MMD, an epidemic of MMD is expected in the near future, especially in East Asian countries where the prevalence of high myopia is 7% to 22% (1–3). Although our knowledge of the pathologic changes in high myopia has advanced since the past decade, a lot is still unknown about the pathogenesis of MMD. One of the unmet needs in the clinical management of high myopia lies in predicting those who are at the greatest risk of MMD progression. This may now be possible with advances in imaging technology that have enabled the *in vivo* study of the retina/choroid/sclera complex, some or all of which are likely to be the primary protagonists in the pathogenesis of MMD (1, 4–6).

The advent of optical coherence tomographic angiography (OCTA) enabled imaging of the choroidal vasculature non-invasively, making it possible to assess the choroid beyond the single dimension of choroidal thickness. Our group had previously utilized swept source optical coherence tomography (SS-OCT) to identify decreased choroidal thickness (CT) as a key feature in MMD, and demonstrated that CT was more strongly associated with MMD than scleral thickness (7). This finding suggests that analysis of the choroidal layer may provide further clues to the pathogenesis of MMD. However, it was still unclear if choroidal thinning in MMD stems from atrophy of the choroidal vasculature or stroma.

OCTA remains limited in the visualization of the deeper vascular layers of the choroid, mostly because of scattering by the pigment in the RPE and by vessels in the choriocapillaris (CC), and consequent signal attenuation (8). Moreover, the CC produces strong OCTA projection artifacts in the underlying choroid. Because of the signal attenuation, choroidal vessels are typically visualized as silhouettes with complete loss of signal at greater depths. Consistent visualization of the medium and larger-sized vessels of Sattler's and Haller's layers may be better appreciated in eyes with areas of overlying RPE loss or depigmentation with absence of the CC, permitting greater penetration of light into the choroid.

Currently, these limitations have been partially overcome by using ultrahigh-speed SS-OCTA instruments (9). Recently, the choroid has been imaged with a novel research device with a Fourier-domain mode-locked laser system operating with a 1.7-MHz sweep rate (1.7 million A-scans/s), at a 1065-nm center wavelength. In a recent study, this device was used to obtain OCTA images with a phase-variance method and these images were qualitatively compared with those obtained with an SD-OCTA instrument operating with a 68 kHz imaging rate and an 840-nm center wavelength (10). In this comparison, the authors noted an improved visualization of the medium and larger-sized choroidal vessels in the images obtained using the SS-OCTA with increased imaging speed. Notably, the visualization of the choroid with this device was demonstrated to be even better than that obtained with ICGA, since the latter imaging modality does not resolve the meshwork of capillary vessels and has limited capability to visualize the medium-sized vessels. However, given these limitations in the visualization of the deeper choroidal vascular layers using existing commercial instruments, most OCTA studies thus far have focused on the CC, providing the greatest amount of information for this thin dense layer of capillaries, both in healthy and affected eyes.

Similarly in one of our follow-up study, we demonstrated qualitatively the presence of choriocapillaris signal voids on OCTA in eyes with MMD (11). The degree of choriocapillaris signal voids was more extensive than that indicated by the severity of MMD, suggesting that OCTA evaluation of the CC may detect pathological changes before the onset of clinically apparent atrophy. We postulated that choriocapillaris changes suggest that the pathogenesis of MMD may be related to the Bruch's membrane, which is essentially the basement membrane of the choriocapillaris. However, we did not evaluate changes in the deeper layers of the choroid, namely the Sattler's and Haller's layers, and whether vascular changes in these deeper layers could be the cause of alterations in the choriocapillaris. To address this, our group developed a novel segmentation technique correlating OCTA images and the anatomical OCT structure of the choroid that allowed the detailed vascular analysis of Haller's and Sattler's layers in high myopes (11).

In this study, we aim to evaluate changes in the medium and large choroidal vessel layers of high myopes with MMD using the aforementioned technique.

Methods

Study population

This was a clinic-based observational clinical study in which patients with high myopia aged 21-70 years, with manifest spherical equivalent (SE) of ≤ -5.0 dioptres (D) or axial length (AL) of ≥ 25mm in either eye, were recruited from the High Myopia clinic of the Singapore National Eye Centre from January 2017 to December 2017. Both eyes of a patient may be included for analysis if the eye has a SE of ≤ -5.0 D or AL of ≥ 25mm. Patients with any coexisting or previous ocular disease in either eye, including corneal opacities, uveitis, dense cataracts, vitreous haemorrhage, diabetic retinopathy or diabetic macular edema, central serous chorioretinopathy, previous retinal laser photocoagulation or photodynamic therapy, previous and coexisting retinal detachment, retinal dystrophies, macular scarring from any cause other than myopic maculopathy, retinopathy due to any cause other than myopia, previous retinal vein or artery occlusion, and ocular ischemic syndrome were excluded from this study. This study was approved by the Centralized Institutional Review Board (CIRB) of SingHealth, Singapore (protocol number R1364/50/2016) and conducted in accordance with the Declaration of Helsinki. All participants provided signed informed consent for their participation.

Clinical examination

All patients underwent comprehensive ophthalmic evaluation including best corrected visual acuity (BCVA), measured with the logarithm of the minimal angle of resolution (logMAR) chart (Lighthouse International, New York, New York, USA) at 4 meters, slit lamp biomicroscopy examination, and manifest refraction performed by certified study optometrists. Intraocular pressure was measured with Goldmann applanation tonometry. Spherical equivalent (SE) was calculated as the sum of the spherical power and half of the cylindrical power. The IOL Master (Carl Zeiss Meditec AG, Jena, Germany) was used for ocular biometry including AL, anterior chamber depth (ACD) and keratometry measurements.

Imaging protocol and image grading

Fundus photography centered at the fovea was performed with a 45-degree digital retinal camera after pupillary dilation with tropicamide 1% and phenylephrine 2.5%, using Canon CR-DGi with Canon EOS 10D SLR backing (Canon Inc, Tokyo, Japan). The optical coherence tomography (OCT) images were obtained using a swept source OCT device (Topcon DRI OCT Triton, Topcon, Tokyo, Japan). This instrument uses a light source with a central wavelength of 1050 nm and an acquisition speed of 100,000 A scans per second. 12mm raster and radial scans centered on the macula and optic nerve were obtained. Fundus photographs and OCT images were graded by 2 retinal specialists (CWW, QVH) for retinal and optic nerve lesions.

Grading of MMD

Two retinal specialists (CWW, QVH), masked to participant characteristics performed grading of the fundus photographs using the International Meta-Analysis for Pathologic Myopia classification.

Segmentation of choroidal layers

3mm×3mm images from the Plex Elite (PLEX Elite, Carl Zeiss Meditec, Dublin, CA) were used for the analysis of choroidal layers. The highest-quality foveal cut of the OCT B-scans was chosen by two experienced fellowship-trained retinal specialists (CWW and QVH) for choroidal thickness grading. Only one highest-quality B-scan, closest to the foveal center was used for segmentation. The choroid was manually segmented by two masked observers, with excellent reliability (ICC = 0.987) into overall choroidal layer (CL), medium-vessel choroidal layer (MVCL), and large-vessel choroidal layer (LVCL) according to the technique described by Devarajan et al., 2019 (11). Using the PLEX Elite software, the choriocapillaris layer presented with default segmentation lines close to the Bruch's membrane (Figure 1). CL was segmented by adjusting the top segmentation line to the Bruch's membrane – for images where the default segmentation lines are at the wrong position – and moving the
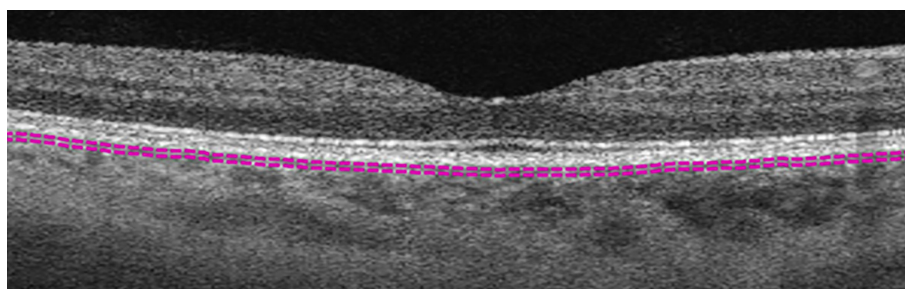

FIGURE 1
Example of choriocapillaris layer marked by default segmentation lines (purple dashed lines).

bottom segmentation line to the suprachoroid, which is indicated by the lowest visible large vessel (Figure 2). MVCL was segmented next by moving the bottom segmentation line above the highest point of the hyporeflective large vessels, leaving MVCL with a hyperreflective appearance comprising of the small and medium vessels of the Sattler's layer (Figure 3). LVCL segmentation was performed by subtracting MVCL from CL, giving this layer the appearance of only hyporeflective large vessels of the Haller's layer (Figure 4). The thickness of each layer was calculated by subtracting the value of the top segmentation line from the bottom segmentation line (in µm). Eyes with overall choroidal thickness less than 100 µm were excluded as it was not possible to have reliable segmentation of the choroid into the MVCL and LVCL sublayers.

Enface images obtained from segmenting the different layers were compiled and processed using Matlab as described by Devarajan et al., 2019 (11) for choroidal vasculature parameters: choroidal vessel density (CVD, %), choroidal branch area (CBA, %), and mean choroidal vessel width (MCVW, µm) see Figure 5.

A total of 12 choroidal vascular parameters were obtained: overall choroidal layer thickness (CT_{CL}), medium-vessel choroidal layer thickness (CT_{MVCL}), large-vessel choroidal layer thickness (CT_{LVCL}), choroidal vessel density – overall choroidal layer (CVD_{CL}), choroidal vessel density – medium-vessel choroidal layer (CVD_{MVCL}), choroidal vessel density – large-vessel choroidal layer (CVD_{LVCL}), choroidal branch area – overall choroidal layer (CBA_{CL}), choroidal branch area – medium-vessel choroidal layer (CBA_{MVCL}), choroidal branch area – large-vessel choroidal layer (CBA_{LVCL}), mean choroidal vessel width – overall choroidal layer ($MCVW_{CL}$), mean choroidal vessel width – medium-vessel choroidal layer ($MCVW_{MVCL}$), and mean choroidal vessel width – large-vessel choroidal layer ($MCVW_{LVCL}$).

Statistical analysis

All data were expressed as mean ± standard deviation or proportions as appropriate. Means were compared with the two-sample Kolmogorov-Smirnov test. Binary logistic regression analysis was performed to identify independent factors associated with poorer visual acuity, adjusted for age. Each individual's left and right eye was accounted for as fixed effects. Each choroidal morphometric vascular parameter was corrected for magnification error calculated using Littman's method and the Bennett formula, $F = 3.48 \times 0.01306 \times (AL - 1.82)$, where F represents the magnification factor and AL represents axial length. A p-value of <0.05 was considered to be statistically significant. All statistical analyses were performed using Stata/MP 16.1 (College Station, TX 77845, USA).

Results

In the original cohort, there were very few eyes that were META-PM category 3 or 4 (five and two, respectively). In addition, we were also unable to segment the choroid into sublayers for such eyes with very thin choroids. We therefore excluded the META-PM category 3 and 4 eyes. A total of 148 eyes were included and were split into two groups for analysis, with 74 eyes in the MMD2 group and 74 eyes in the no MMD group.

Patients with MMD2 were significantly older (56.4 ± 12.0 vs. 51.2 ± 12.2 years, p = 0.009) and had longer AL (29.0 ± 1.6 vs. 27.4 ± 1.4 mm, p < 0.001) than those without see Table 1.

Age and 12 choroidal vascular parameters were analysed for any significant correlation with AL, BCVA and CT. Longer AL was associated with thinner CT_{CL} (r = -0.58, p < 0.001), thinner CT_{MVCL} (r = -0.22, p = 0.04), lower CVD_{CL} (r = -0.19, p = 0.02), reduced $MCVW_{CL}$ (r = -0.58, p < 0.001), and greater CBA_{CL} (r = 0.61, p < 0.001). Poorer BCVA was associated with thinner CT_{CL} (r = -0.21, p = 0.01). Thinner CT_{CL} was also associated with older age (r = -0.38, p < 0.001), and greater CBA_{CL} (r = -0.60, p < 0.001) with an equal increase in CBA_{MVCL} and CBA_{LVCL} (r = -0.22, p = 0.04 for both). Thinner CT_{CL} was also associated with thinner CT_{MVCL} (r = 0.79, p < 0.001) and CT_{LVCL} (r = 0.98, p < 0.001), decreased CVD_{CL} (r = 0.38, p < 0.001) with significant decrease in CVD_{LVCL} (r = 0.41, p < 0.001), and reduced $MCVW_{CL}$ (r = 0.61, p < 0.001) also with significant decrease in $MCVW_{LVCL}$ (r = 0.27, p = 0.01) but the changes for CVD_{MVCL} and $MCVW_{MVCL}$ were not considered as significant (p ≥ 0.05) (Table 2).

Comparison of the choroidal vascular parameters between eyes with MMD2 and with no MMD revealed that eyes with MMD2
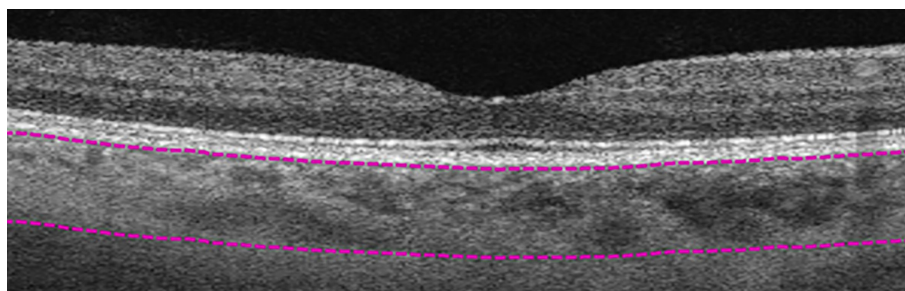

FIGURE 2
Manual segmentation of overall choroidal layer (CL). Top segmentation line (top purple dashed line) sits at the innermost border of the choroidal layer, while the bottom segmentation line (lower purple dashed line) was shifted to the outermost large choroidal vessel, marking the CL as the layer between the purple segmentation lines.
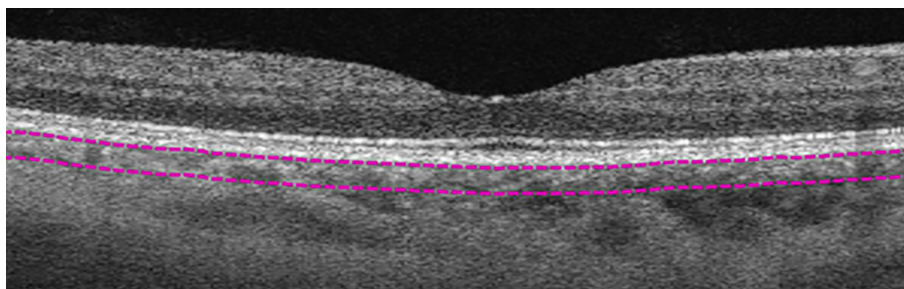
FIGURE 3
Manual segmentation of medium-vessel choroidal layer (MVCL). Top segmentation line (top purple dashed line) sits at the innermost border of the choroidal layer, while the bottom segmentation line (lower purple dashed line) was shifted to the innermost large choroidal vessel, marking the MVCL between the purple dashed segmentation lines.

have thinner CT_{CL} (120.37±47.18μm vs 218.33±92.70μm, p<0.001), along with thinner CT_{MVCL} (70.57±15.28μm vs 85.32±23.71μm, p=0.04) and CT_{LVCL} (101.65±25.36μm vs 154.55±68.41μm, p=0.001). But had greater CVD_{CL} (71.10±3.97% vs 66.97±3.63%, p<0.001), CVD_{MVCL} (66.96±2.35% vs 65.06±2.69%, p=0.002), CVD_{LVCL} (68.36±2.56% vs 66.58±2.88%, p=0.012), $MCVW_{MVCL}$ (6.14±0.34μm vs 5.90±0.35μm, p=0.007), and greater CBA_{CL} (12.69 ±1.38% vs 11.34±1.18%, p<0.001) in eyes with MMD2 (Table 3).

Binary logistic regression, prior to adjusting for age (unadjusted odds ratio), revealed thicker CT_{CL} (odds ratio (OR) 0.98, 95% confidence interval (CI) 0.97-0.98, p < 0.001), thicker CT_{MVCL} (OR 0.96, 95% CI 0.94-0.99, p = 0.001) and thicker CT_{LVCL} (OR 0.97, 95% CI 0.96-0.98, p < 0.001) were associated with lower odds of MMD2. Presence of MMD2 was associated with greater odds of increased CVD_{CL} (OR 1.35, 95% CI 1.20-1.53, p < 0.001), increased CVD_{MVCL} (OR 1.34, 95% CI 1.10-1.63, p = 0.004), increased CVD_{LVCL} (OR 1.26, 95% CI 1.05-1.51, p = 0.01), increased CBA_{CL} (OR 2.25, 95% CI 1.60-3.17, p < 0.001) and increased $MCVW_{MVCL}$ (OR 6.79, 95% CI 1.53-30.22, p = 0.01). After adjusting for age (adjusted odds ratio), thicker CT_{CL} (OR 0.98, 95% CI 0.97-0.99, p < 0.001), thicker CT_{MVCL} (OR 0.97, 95% CI 0.94-0.99, p = 0.002) and thicker CT_{LVCL} (OR 0.97, 95% CI 0.96-0.98, p < 0.001) remained associated with lower odds of MMD2. Presence of MMD2 remained significantly associated with greater odds of increased CVD_{CL} (OR 1.37, 95% CI 1.20-1.55, p < 0.001), increased CVD_{MVCL}

(OR 1.39, 95% CI 1.12-1.73, p = 0.003), increased CVD_{LVCL} (OR 1.31, 95% CI 1.07-1.60, p = 0.009), increased CBA_{CL} (OR 2.19, 95% CI 1.55-3.08, p < 0.001) and increased $MCVW_{MVCL}$ (OR 6.97, 95% CI 1.59-30.51, p = 0.01) (Table 4).

Discussion

Consistent with previous studies (12–14), our study found a strong correlation between AL and CT, where the longer the AL, the thinner the CT_{CL} (r = -0.58, p < 0.001). Besides CT_{CL}, CVD_{CL} (r = -0.19, p = 0.02) and $MCVW_{CL}$ (r = -0.58, p < 0.001) were also noted to decrease with longer AL, while CBA_{CL} increases with longer AL (r = 0.61, p < 0.001). None of the parameters for the middle- and large-vessel choroidal layers, except for CT_{MVCL} (r = -0.22, p = 0.04) were significantly associated with changes in AL. Other investigators had noted similar findings for the negative correlation for CT_{CL}, CVD_{CL} and $MCVW_{CL}$ with AL, and positive correlation for CBA_{CL} with AL (15–18). Taken together, these findings suggest that the increase in AL could have exerted a stretching force on the choroidal vessels, thereby decreasing choroidal vessel width. With the decrease in vessel width, there would be a decrease in blood flow which would affect the choroidal thermoregulation (19). Thus, this could have led to the increase in CBA, which could be an increase in choroidal vascular branching or
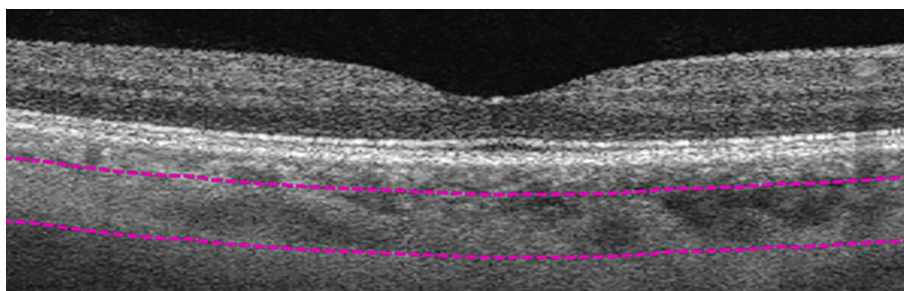

FIGURE 4
Manual segmentation of large-vessel choroidal layer (LVCL). Top segmentation line (top purple dashed line) sits at the innermost large choroidal vessel, while the bottom segmentation line (lower purple dashed line) was shifted to the outermost large choroidal vessel, marking the LVCL between the purple dashed segmentation lines.
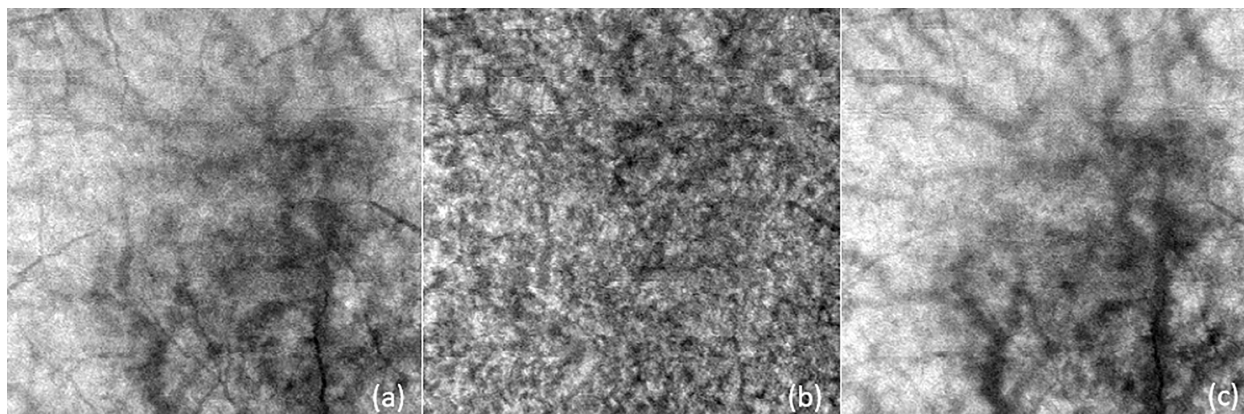
FIGURE 5
Examples of enface images for **(A)** overall choroidal layer (CL), **(B)** medium vessel choroidal layer (MVCL), and **(C)** large vessel choroidal layer (LVCL). These images were subsequently processed with Matlab for choroidal vasculature parameters: choroidal vessel density (CVD), choroidal branch area (CBA), and mean choroidal vessel width (MCVW).

elongation or both, in an attempt by the eye to regulate the retinal/ choroidal blood supply, similar to the mechanism where choroidal neovascularisation (CNV) occurs. Interestingly, blood flow in choroidal vessels has been reported to be lower in highly myopic versus non-highly myopic eyes, with a possible negative correlation between axial length and choroidal blood flow [20]. This supports the idea that the thinning of MCVW could have led to a noticeable decrease in blood flow and vessel branching increase could be a compensatory mechanism to overcome the limitation in blood flow. Further investigation is necessary to verify if the molecular mechanisms of choroidal vessel changes in elongated, pathological eyes have any similarities to CNV.

Thinner CT_{CL} was also associated with worse BCVA (r = -0.21, p = 0.01), older age (r = -0.38, p < 0.001), and thinner CT_{MVCL} and CT_{LVCL} (r = 0.79 and r = 0.98, p < 0.001 for both), mirroring what several other groups had observed [12–14, 21, 22]. CVD_{CL} was also noted to be positively correlated with CT_{CL} (r = 0.38, p < 0.001), with the changes in CVD_{LVCL} being the main driver (r = 0.41, p < 0.001). Wang et al. (2020) similarly noted that CVD_{LVCL} was larger in patients with central serous chorioretinopathy (CSC) as compared to controls (62.3 ± 6.6% vs. 54.1 ± 8.0%, p = 0.02) [23]. Although these eyes were affected by a different disease, it seems that regardless of the type of disease, CVD_{LVCL} appears to play a more impactful role than CVD_{MVCL} for changes in the overall choroidal layer.

Our understanding of the changes in CVD could be further broken down through understanding the changes for CBA and MVCW, with $MCVW_{CL}$ (r = 0.61, p < 0.001) and $MCVW_{LVCL}$ (r = 0.27, p = 0.01) noted to have a significant positive correlation with changes in CT as well. Together with the results for CVD, the large-vessel choroidal layer appears to be a more active player in driving changes for the overall choroidal layer than the medium-vessel choroidal layer as the correlation for CVD_{MVCL} was not significant (p = 0.86) and $MCVW_{MVCL}$ was marginally significant (p = 0.06). For CBA_{CL} (r = -0.60, p < 0.001), it was negatively correlated with CT_{CL}, with equal contributions of both MVCL and LVCL (r = -0.22, p = 0.04 for both) affecting the increase in the choroidal branch area. From the changes in CBA and CVD, it seemed that changes for MCVW were probably larger than that of the choroidal branching (which could either be an increase in vessel branching or increased length of vessels) to result in overall changes in CVD to be similarly negatively correlated with CT changes.

Several choroidal vasculature parameters that we studied (CT_{CL}, CT_{MVCL}, CT_{LVCL}, CVD_{CL}, CVD_{MVCL}, CVD_{LVCL}, CBA_{CL}, and $MCVW_{MVCL}$) were significantly altered in the presence of MMD2 (Table 3). Compared to eyes with no MMD, MMD2 eyes showed thinner CT_{CL} (120.37μm vs 218.33μm, p < 0.001), which was consistent for both MVCL (70.57μm vs 85.32μm, p = 0.04) and LVCL (101.65μm vs 154.55μm, p=0.001). This finding is similar to other studies, in which Wong et al. noted that CT was highly

TABLE 1 Patient characteristics.

	Overall (n=148)	MMD2 (n=74)	No MMD (n=74)	P-value
Age, years	53.8±12.3	56.4±12.0	51.2±12.2	**0.009***
Gender (male), %	39.2%	35.1%	43.2%	0.97
AL, mm	28.2±1.7	29.0±1.6	27.4±1.4	**< 0.001***
logMAR BCVA	0.22±0.16	0.24±0.15	0.21±0.17	0.78

Asterisk and bold font denote P < 0.05. AL, axial length; BCVA, best-corrected visual acuity; MMD, myopic macular degeneration.

TABLE 2 Correlation of age and choroidal vascular parameters with AL, BCVA and CT.

	AL		BCVA		CT_{CL}	
	r	P-value	r	P-value	r	P-value
Age	0.09	0.27	0.12	0.16	-0.38	**< 0.001***
CT_{CL}	-0.58	**< 0.001***	-0.21	**0.01***	–	–
CT_{MVCL}	-0.22	**0.04***	-0.13	0.23	0.79	**< 0.001***
CT_{LVCL}	-0.19	0.81	-0.21	0.05	0.98	**< 0.001***
CVD_{CL}	-0.19	**0.02***	-0.15	0.07	0.38	**< 0.001***
CVD_{MVCL}	-0.19	0.08	0.13	0.22	0.02	0.86
CVD_{LVCL}	-0.08	0.46	-0.06	0.60	0.41	**<0.001***
CBA_{CL}	0.61	**< 0.001***	0.01	0.88	-0.60	**< 0.001***
CBA_{MVCL}	0.19	0.07	-0.18	0.10	-0.22	**0.04***
CBA_{LVCL}	0.18	0.09	-0.04	0.72	-0.22	**0.04***
$MCVW_{CL}$	-0.58	**< 0.001***	-0.03	0.68	0.61	**< 0.001***
$MCVW_{MVCL}$	-0.19	0.07	0.19	0.08	0.21	0.06
$MCVW_{LVCL}$	-0.18	0.09	0.02	0.82	0.27	**0.01***

Each choroidal morphometric vascular parameter was corrected for magnification error. Asterisk and bold font denote P < 0.05. AL, axial length; BCVA, best-corrected visual acuity; CBA, choroidal branch area; CL, overall choroidal layer; CT, choroidal layer thickness; CVD, choroidal vessel density; LVCL, large-vessel choroidal layer; MCVW, mean choroidal vessel width; MVCL, medium-vessel choroidal layer. Magnification error was calculated using Littman's method and the Bennett formula $F = 3.48 \times (AL\text{-}1.82)$, where F represents the magnification factor and AL represents axial length.

correlated to MMD [7], and Zhou et al. similarly noted that CT is thinner in more myopic eyes [24]. Meanwhile, Zhao et al. also found that MVCL was only significantly associated with a higher prevalence of some, and not all, macular diseases [14].

Interestingly, it was noted by Yang and Koh that impediment of ocular blood was possibly associated with axial length increase, especially so in high myopes [20]. In the present study, we find three choroidal vascular parameters that may reflect worsened hypoxia (Table 3). For example, compared to eyes with no MMD, choroidal vessel density was consistently higher in MMD2 eyes for CVD_{CL} (71.10 vs. 66.97%, p < 0.001) as well as for CVD_{MVCL} and CVD_{LVCL} (p = 0.002 and p = 0.012). Moreover, $MCVW_{MVCL}$ was greater in MMD2 eyes versus eyes with no MMD (6.14 vs. 5.90 μm, p = 0.007). Additionally, the choroidal branching area (CBA_{CL}) was

TABLE 3 Comparison of choroidal vascular parameters between eyes with MMD2 versus no MMD.

	Overall (n=148)	MMD2 (n=74)	No MMD (n=74)	P-value*
CT_{CL}	169.35±88.25	120.37±47.18	218.33±92.70	**< 0.001***
**CT_{MVCL}	80.84±22.48	70.57±15.28	85.32±23.71	**0.04***
**CT_{LVCL}	138.50±63.50	101.65±25.36	154.55±68.41	**0.001***
CVD_{CL}	69.03±4.32	71.10±3.97	66.97±3.63	**<0.001***
CVD_{MVCL}	65.62±2.73	66.96±2.35	65.06±2.69	**0.002***
CVD_{LVCL}	67.11±2.89	68.36±2.56	66.58±2.88	**0.012***
CBA_{CL}	12.02±1.45	12.69±1.38	11.34±1.18	**< 0.001***
CBA_{MVCL}	12.74±0.89	12.88±0.93	12.68±0.88	0.15
CBA_{LVCL}	10.52±0.97	10.81±0.94	10.40±0.97	0.13
$MCVW_{CL}$	6.91±0.44	6.94±0.42	6.89±0.46	0.29
$MCVW_{MVCL}$	5.97±0.36	6.14±0.34	5.90±0.35	**0.007***
$MCVW_{LVCL}$	7.42±0.62	7.50±0.68	7.39±0.60	0.93

Means of the MMD2 group and no MMD group were compared using the two-sample Kolmogorov-Smirnov test. Each choroidal morphometric vascular parameter was corrected for magnification error. Asterisk and bold font denote P < 0.05. **N=62 for the No-MMD group and N=27 for the MMD2 group for MVCL and LVCL comparisons. CBA = choroidal branch area. CL, overall choroidal layer; CT, choroidal layer thickness; CVD, choroidal vessel density; LVCL, large-vessel choroidal layer; MCVW, mean choroidal vessel width; MMD, myopic macular degeneration; MVCL, medium-vessel choroidal layer. Magnification error was calculated using Littman's method and the Bennett formula $F = 3.48 \times 0.01306 \times (AL\text{-}1.82)$, where F represents the magnification factor and AL represents axial length.

TABLE 4 Association of choroidal vascular parameters with presence of MMD2.

	Unadjusted Odds ratio	95% CI	P-value	Adjusted odds ratio	95% CI	P-value
CT_{CL}	0.98	0.97-0.98	**< 0.001***	0.98	0.97-0.99	**< 0.001***
CT_{MVCL}	0.96	0.94-0.99	**0.001***	0.97	0.94-0.99	**0.002***
CT_{LVCL}	0.97	0.96-0.98	**< 0.001***	0.97	0.96-0.98	**<0.001***
CVD_{CL}	1.35	1.20-1.53	**< 0.001***	1.37	1.20-1.55	**<0.001***
CVD_{MVCL}	1.34	1.10-1.63	**0.004***	1.39	1.12-1.73	**0.003***
CVD_{LVCL}	1.26	1.05-1.51	**0.01***	1.31	1.07-1.60	**0.009***
CBA_{CL}	2.25	1.60-3.17	**< 0.001***	2.19	1.55-3.08	**<0.001***
CBA_{MVCL}	1.29	0.75-2.24	0.36	1.35	0.78-2.33	0.29
CBA_{LVCL}	1.58	0.94-2.67	0.09	1.54	0.91-2.61	0.11
$MCVW_{CL}$	1.36	0.64-2.86	0.42	1.65	0.73-3.76	0.23
$MCVW_{MVCL}$	6.79	1.53-30.2	**0.01***	6.97	1.59-30.51	**0.01***
$MCVW_{LVCL}$	1.32	0.62-2.81	0.47	1.45	0.67-3.17	0.35

"Adjusted odds ratio" was adjusted for age. Each choroidal morphometric vascular parameter was corrected for magnification error. Each individual's left and right eye was accounted for as fixed effects. Asterisk and bold font denote P < 0.05. CBA, choroidal branch area; CL, overall choroidal layer; CT, choroidal layer thickness; CVD, choroidal vessel density; LVCL, large-vessel choroidal layer; MCVW, mean choroidal vessel width; MVCL, medium-vessel choroidal layer; Magnification error was calculated using Littman's method and the Bennett formula, $F = 3.48 \times 0.01306 \times (AL$-1.82), where F represents the magnification factor and AL represents axial length.

significantly greater in eyes with MMD2 (12.69 vs. 11.34%, p < 0.001). As discussed further below, hypoxia, specifically in the choriocapillaris layer could readily result in a compensatory response in medium- as well as the large-vessel layers in attempts improve perfusion with increased vessel density, increased vessel width and increased branching area.

Thicker CT_{CL}, with significant contributions from both MVCL and LVCL, were significantly associated with lower odds of MMD2, after adjusting for age (OR 0.98, 95% CI 0.97-0.99, p < 0.001; OR 0.97, 95% CI 0.94-0.99, p = 0.002; OR 0.97, 95% CI 0.96-0.98, p < 0.001, respectively). As mentioned above, a compensatory response to hypoxia in the choriocapillaris likely explains our finding that presence of MMD2 increases the odds of higher CVD (of CL, MVCL and LVCL), CBA_{CL} and $MCVW_{MVCL}$. Another possible explanation for the increase in CVD could be the increased risk of myopic complications in MMD eyes. MMD eyes are known to have a higher risk of developing posterior staphylomas and myopic CNV, with both features being associated with pronounced choroidal thinning (19, 25, 26). Limitations in discerning the individual choroidal layers within staphyloma eyes leave open the possibility of an increased CVD within the MVCL and LVCL as some sort of defense mechanism which the eye could have taken to prevent staphyloma formation/progression. As the choriocapillaris is not readily resolvable in standard OCTA imaging, it could very well be the changes in the MVCL and LVCL mask changes occurring in the much thinner choriocapillaris, which would contribute relatively less to the overall change in the CL. Also, as it is currently unknown which choroidal layer myopic neovascularization originates from (19), we cannot eliminate the possibility of mCNV originating from the MVCL or LVCL versus the choroicapillaris. With overall thinning of the choroid in MMD eyes, the increase in CVD_{MVCL} and CVD_{LVCL} could be a defensive mechanism where the choroid tries to regulate choroidal blood flow to prevent hypoxia. Similarly, an increase in vessel width

($MCVW_{MVCL}$) could be a similar defense mechanism. Moreover, past studies have suggested that a response to hypoxia could be increased vessel branching (27). Increased branching would result in increased CVD. Hypoxia may very well explain why the presence of MMD increases the odds of greater CBA, CVD and MCVW.

Our study is not without its limitations, some of which are discussed above. In the original cohort, there were very few eyes that were META-PM category 3 or 4 (five and two, respectively). In addition, we were also unable to segment the choroid into the MVCL and LVCL sublayers for such eyes which would have extremely thin choroids. We therefore excluded the META-PM category 3 and 4 eyes. Hence, this study was not designed to assess the effect of MMD severity, and we could only assess the effect of its presence. Furthermore, our study has a cross-sectional design and this precludes the inference of a temporal or sequential relationship. In this regard, we cannot tell which choroidal layer the main changes in axial elongation occur in. Moreover, we did not account for chronic conditions such as diabetes, kidney disease and hypertension. These conditions are associated with changes in the choroidal vasculature (20), which could lead to a different interpretation of results if they were taken into account. Also, questions remain on whether choroidal vessels appeared thinner mainly due to the mechanical stretching forces or if they were congenitally thinner in eyes with a higher risk of myopia (28). Histological studies had revealed that the choroid thins with age and increased refractive error, but the cause of choroidal thinning remains poorly understood. Comparing choroidal thickness in similar AL could provide a better idea of how different the choroidal vessels are. Staphyloma, mCNV and other MMD-related features were not investigated in this study as well, which could have provided us with a better idea of why CVD_{MVCL} increases with an increase in odds of MMD.

In conclusion, longer eyes were observed to have decreased choroidal vessel width, reduced choroidal vessel density, thinner

choroidal layer, and increased vascular branching. The latter could be a compensatory mechanism to maintain choroidal blood supply in elongated eyes. A thinner choroid, with almost equal MVCL and LVCL thinning, and denser MVCL, which may be signs of hypoxia, were also associated with greater odds of MMD.

Data availability statement

The raw data supporting the conclusions of this article will be made available by the authors, without undue reservation.

Ethics statement

The studies involving human participants were reviewed and approved by Centralized Institutional Review Board (CIRB) of SingHealth, Singapore. The patients/participants provided their written informed consent to participate in this study.

Author contributions

YD and KC drafted the manuscript. SL performed all statistical analysis and created all tables. QW helped acquire the data. RC, CW and QH conceived the project, acquired the data and directed the writing and analysis. All authors proofread the manuscript. All authors contributed to the article and approved the submitted version.

Conflict of interest

The authors declare that the research was conducted in the absence of any commercial or financial relationships that could be construed as a potential conflict of interest.

Publisher's note

All claims expressed in this article are solely those of the authors and do not necessarily represent those of their affiliated organizations, or those of the publisher, the editors and the reviewers. Any product that may be evaluated in this article, or claim that may be made by its manufacturer, is not guaranteed or endorsed by the publisher.

References

1. Saw SM, Matsumura S, Hoang QV. Prevention and management of myopia and myopic pathology. *Invest Ophthalmol Vis Sci* (2019) 60(2):488. doi: 10.1167/iovs.18-25221

2. Ohno-Matsui K, Wu PC, Yamashiro K, Vutipongsatorn K, Fang Y, Cheung CMG, et al. IMI pathologic myopia. *Invest Ophthalmol Vis Sci* (2021) 62(5):5. doi: 10.1167/iovs.62.5.5

3. Holden BA, Fricke TR, Wilson DA, Jong M, Naidoo KS, Sankaridurg P, et al. Global prevalence of myopia and high myopia and temporal trends from 2000 through 2050. *Ophthalmology* (2016) 123(5):1036–42. doi: 10.1016/j.ophtha.2016.01.006

4. Saw SM, Chua WH, Hong CY, Wu HM, Chan WY, Chia KS, et al. Nearwork in early-onset myopia. *Invest Ophthalmol Vis Sci* (2002) 43(2):332–9.

5. French AN, Morgan IG, Mitchell P, Rose KA. Patterns of myopigenic activities with age, gender and ethnicity in Sydney schoolchildren. *Ophthalmic Physiol Opt* (2013) 33(3):318–28. doi: 10.1111/opo.12045

6. Mutti DO, Mitchell GL, Moeschberger ML, Jones LA, Zadnik K. Parental myopia, near work, school achievement, and children's refractive error. *Invest Ophthalmol Vis Sci* (2002) 43(12):3633–40.

7. Wong CW, Phua V, Lee SY, Wong TY, Cheung CMG. Is choroidal or scleral thickness related to myopic macular degeneration? *Invest Ophthalmol Vis Sci* (2017) 58 (2):907. doi: 10.1167/iovs.16-20742

8. Diaz JD, Wang JC, Oellers P, Lains I, Sobrin L, Husain D, et al. Imaging the deep choroidal vasculature using spectral domain and swept source optical coherence tomography angiography. *J VitreoRetinal Diseases* (2018) 2(3):146–54. doi: 10.1177/2474126418771805

9. Choi W, Mohler KJ, Potsaid B, Lu CD, Liu JJ, Jayaraman V, et al. Choriocapillaris and choroidal microvasculature imaging with ultrahigh speed OCT angiography. *Wedrich A Ed PloS One* (2013) 8(12):e81499. doi: 10.1371/journal.pone.0081499

10. Poddar R, Migacz JV, Schwartz DM, Werner JS, Gorczynska I. Challenges and advantages in wide-field optical coherence tomography angiography imaging of the human retinal and choroidal vasculature at 1.7-MHz a-scan rate. *J BioMed Opt* (2017) 22(10):106018. doi: 10.1117/1.JBO.22.10.106018

11. Devarajan K, Sim R, Chua J, Wong CW, Matsumura S, Htoon HM, et al. Optical coherence tomography angiography for the assessment of choroidal vasculature in high myopia. *Br J Ophthalmol* (2020) 104(7):917–23. doi: 10.1136/bjophthalmol-2019-314769

12. Flores-Moreno I, Lugo F, Duker JS, Ruiz-Moreno JM. The relationship between axial length and choroidal thickness in eyes with high myopia. *Am J Ophthalmol* (2013) 155(2):314–319.e1. doi: 10.1016/j.ajo.2012.07.015

13. Nishida Y, Fujiwara T, Imamura Y, Lima LH, Kurosaka D, Spaide RF. Choroidal thickness and visual acuity in highly myopic eyes. *Retina* (2012) 32(7):1229–36. doi: 10.1097/IAE.0b013e318242b990

14. Zhao J, Wang YX, Zhang Q, Wei WB, Xu L, Jonas JB. Macular choroidal small-vessel layer, sattler's layer and haller's layer thicknesses: the Beijing eye study. *Sci Rep* (2018) 8(1):4411. doi: 10.1038/s41598-018-22745-4

15. Alshareef RA, Khuthaila MK, Januwada M, Goud A, Ferrara D, Chhablani J. Choroidal vascular analysis in myopic eyes: evidence of foveal medium vessel layer thinning. *Int J Retin Vitr* (2017) 3(1):28. doi: 10.1186/s40942-017-0081-z

16. Sato M, Minami S, Nagai N, Suzuki M, Kurihara T, Shinojima A, et al. Association between axial length and choroidal thickness in early age-related macular degeneration. *PloS One* (2020) 15(10):e0240357. doi: 10.1371/journal.pone.0240357

17. Shiihara H, Sakamoto T, Terasaki H, Kakiuchi N, Shinohara Y, Tomita M, et al. Running pattern of choroidal vessel in en face OCT images determined by machine learning–based quantitative method. *Graefes Arch Clin Exp Ophthalmol* (2019) 257 (9):1879–87. doi: 10.1007/s00417-019-04399-8

18. Gao J, Rao CH, Li F, Liu L, Liu KJ. Ultra-widefield swept-source optical coherence tomography angiography in the assessment of choroidal changes in young adults with myopia. *Transl Vis Sci Technol* (2022) 11(12):14. doi: 10.1167/tvst.11.12.14

19. Brinks J, van Dijk EHC, Klaassen I, Schlingemann RO, Kielbasa SM, Emri E, et al. Exploring the choroidal vascular labyrinth and its molecular and structural roles in health and disease. *Prog Retinal Eye Res* (2022) 87:100994. doi: 10.1016/j.preteyeres.2021.100994

20. Yang YS, Koh JW. Choroidal blood flow change in eyes with high myopia. *Korean J Ophthalmol* (2015) 29(5):309. doi: 10.3341/kjo.2015.29.5.309

21. Nivison-Smith L, Khandelwal N, Tong J, Mahajan S, Kalloniatis M, Agrawal R. Normal aging changes in the choroidal angioarchitecture of the macula. *Sci Rep* (2020) 10(1):10810. doi: 10.1038/s41598-020-67829-2

22. Cheong KX, Lim LW, Li KZ, Tan CS. A novel and faster method of manual grading to measure choroidal thickness using optical coherence tomography. *Eye (Lond)* (2018) 32(2):433–8. doi: 10.1038/eye.2017.210

23. Wang E, Zhao X, Yang J, Chen Y. Visualization of deep choroidal vasculatures and measurement of choroidal vascular density: a swept-source optical coherence tomography angiography approach. *BMC Ophthalmol* (2020) 20(1):321. doi: 10.1186/s12886-020-01591-x

24. Zhou Y, Song M, Zhou M, Liu Y, Wang F, Sun X. Choroidal and retinal thickness of highly myopic eyes with early stage of myopic chorioretinopathy: tessellation. *J Ophthalmol* (2018) 2018:1–9. doi: 10.1155/2018/2181602

25. Lu X, Zhang G, Cen L, Du Y, Liu L, Jin C, et al. Choroidal vascular density quantification in high myopia with or without choroidal neovascularization using

optical coherence tomography angiography. *J Ophthalmol* (2023) 2023:1504834. doi: 10.1155/2023/1504834

26. Barteselli G, Lee SN, El-Emam S, Hou H, Ma F, Chhablani J, et al. Macular choroidal volume variations in highly myopic eyes with myopic traction maculopathy and choroidal neovascularization. *Retina* (2014) 34(5):880–9. doi: 10.1097/IAE.0000000000000015

27. Mirzapour-Shafiyi F, Kametani Y, Hikita T, Hasegawa Y, Nakayama M. Numerical evaluation reveals the effect of branching morphology on vessel transport properties during angiogenesis. *PloS Comput Biol* (2021) 17(6):e1008398. doi: 10.1371/journal.pcbi.1008398

28. Shiihara H, Sonoda S, Terasaki H, Kakiuchi N, Yamashita T, Uchino E, et al. Quantitative analyses of diameter and running pattern of choroidal vessels in central serous chorioretinopathy by en face images. *Sci Rep* (2020) 10(1):9591. doi: 10.1038/s41598-020-66858-1